Thermochimica Acta 495 (2009) 51–56

Contents lists available at ScienceDirect

Thermochimica Acta

journal homepage: www.elsevier.com/locate/tca

Melt-crystallization behavior and isothermal crystallization kinetics of crystalline/crystalline blends of poly(ethylene terephthalate)/poly(trimethylene terephthalate)

Mingtao Run[a,*], Yanping Hao[b], Chenguang Yao[a]

[a] College of Chemistry & Environmental Science, Hebei University, Baoding 071002, China
[b] College of Economy, Hebei University, Baoding 071002, China

ARTICLE INFO

Article history:
Received 4 December 2008
Received in revised form 26 May 2009
Accepted 29 May 2009
Available online 6 June 2009

Keywords:
PET/PTT blend
Isothermal crystallization kinetics
DSC
Morphology

ABSTRACT

The melt-crystallization and isothermal melt-crystallization kinetics of poly(ethylene terephthalate)/poly(trimethylene terephthalate) blends (PET/PTT) were investigated by differential scanning calorimetry (DSC) and polarized optical microscopy. Although PET and PTT in the binary blends are miscible at amorphous state, they will crystallize individually when cooled from the melt. In the DSC measurements, PET component with higher supercooling degree will crystallize first, and then the crystallite of PET will be the nucleating agent for PTT, which induce the crystallization of PTT at higher temperature. On the other hand, in both blends of PET80/PTT20 and PET60/PTT40, the PET component will crystallize at higher temperature with faster crystallization rate due to the dilute effect of PTT. So the commingled minor addition of one component to another helps to improve the crystallization of the blends. For blends of PET20/PTT80 and PET40/PTT60, isothermal crystallization kinetics evaluated in terms of the Avrami equation suggest different crystallization mechanisms occurred. The more PET content in blends, the fast crystallization rate is. The Avrami exponent, $n = 3$, suggests a three-dimensional growth of the crystals in both blends, which is further demonstrated by the spherulites formed in all blends. The crystalline blends show multiple-melting peaks during heating process.

1. Introduction

Polymer blending is a widely used way to extend the application fields of polymers, which is straightforward, versatile, and relatively inexpensive for creating a new polymeric material. It has been proved that many physical and mechanical properties of the polymers can be significantly improved [1,2]. Poly(trimethylene terephthalate) (PTT) has been receiving much attention because of its outstanding properties, such as good tensile behavior, resilience, outstanding elastic recovery, dyeability, etc. [3,4]. Moreover, it takes an unusual combination of the topping properties of poly(ethylene terephthalate) (PET) and processing characteristics of poly(butylene terephthalate) (PBT). To bring down the cost yet keeping some of its advantageous properties it seems interesting to apply PTT in blends.

There has been much research on the PTT and its blends or copolymers with other polymers [5–18]. Several literatures are concerned on the thermal properties of the binary blend of PTT/PET [5–7]. Supaphol et al. [5] studied the properties of the binary blends of PTT/PET, and suggested that blends were miscible in the amorphous state, and the blend having 50 wt% of PTT showed the lowest apparent degree of crystallinity and the lowest tensile-strength values. Woo and co-worker [6] and Valenti and co-workers [7] also found that PTT/PET blend is fully miscible (in absence of transesterifications) in amorphous state. The claimed miscibility applied to the quenched state of the blends, and not the crystallized domain involving the crystal cells in the crystalline regions because each component will crystallize individually to form co-existed crystals in common spherulites.

In the present study, various PET/PTT blends with different PTT compositions were prepared by co-rotating twin-screw extruder under the same processing conditions. In order to decrease a maximum of the polycondensation reaction between PET and PTT, the limited time of melt-blending was within 2 min. We consider here the effect of composition and temperature on melt-crystallization of the PET/PTT, in terms of the isothermal crystallization and successive melting behavior by DSC measurements.

2. Experimental

2.1. Materials

PTT homopolymer used in this study was supplied in pellet form by Shell Chemicals (USA) with an intrinsic viscosity of

* Corresponding author. Fax: +86 3125079525.
E-mail address: lhbx@hbu.edu.cn (M. Run).

0040-6031/$ – see front matter © 2009 Elsevier B.V. All rights reserved.
doi:10.1016/j.tca.2009.05.018

0.92 dL/g measured in a phenol/tetrachloroethane solution at 25 °C. PET homopolymer was supplied in pellet form by Tianjin Petrochemical Co. with an intrinsic viscosity of 0.66 dL/g measured in phenol/tetrachloroethane solution at 25 °C.

2.2. Binary blends preparation

The materials were dried in a vacuum oven at 140 °C for 12 h before preparing the blends. The dried pellets of PTT and PET were mixed together with different weight ratios of PET and PTT as follows: B1, 0/100; B2, 20/80; B3, 40/60; B4, 60/40; B5, 80/20; B6, 100/0; next they were melt-blended for about 2 min in a ZSK-25WLE WP self-wiping, co-rotating twin-screw extruder operating at a screw speed of 100 rpm and a die temperature of 280 °C. The resultant blends' ribbons were cooled in cold water, cut up, and re-dried before being used in measurements.

2.3. Differential scanning calorimetry (DSC)

The melt-crystallization of various binary blends was performed by the Perkin–Elmer Diamond DSC instrument that was calibrated with indium prior to performing the measurements; the weights of all samples were approximately 6.0 mg. Samples were heated to 280 °C at 100 °C/min under a nitrogen atmosphere, held for 5 min and then cooled to −50 °C at a constant cooling rate of 10 °C/min. The final cooling scan was recorded. Isothermal crystallization and subsequent melting process were performed as follows: samples were heated at a rate of 100 °C/min to 280 °C, held for 5 min and then cooled to the designated crystallization temperatures (T_c) rapidly (100 °C/min), holding enough time to allow the isothermal crystallization completed; next samples were heated to 280 °C at a rate of 10 °C/min.

2.4. Polarized optical microscopy

Polarized optical microscopy (Yongheng 59XA, China) with a digital camera system (Panasonic wv-CP240, Japan) was used for observation of the crystallites. Samples were prepared by sandwiching a tiny pellet of PET/PTT blend between two glass plates with a film thickness of about 200 μm, compressing at 280 °C for 5 min and then annealing in an oven at 200 °C for 3 h, and then quenched by ice water and dried at room temperature.

3. Results and discussion

3.1. Melt-crystallization characterization

The melt-crystallization behaviors of six samples at the cooling rate of 10 °C/min are shown in Fig. 1; the parameters are listed in Table 1. In the case of crystallization from the melt at a fixed cooling rate, the temperature where the crystallization occurs is mainly determined by supercooling and thus by melting temperature (T_m) of polymers. PET has a higher T_m, and therefore, it can crystallize at a higher temperature, while PTT has a lower T_m and requires further drop in temperature for the occurrence of crystallization.

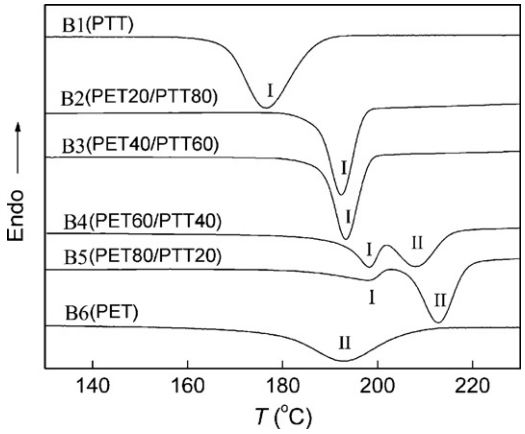

Fig. 1. Melt-crystallization DSC curves of six samples.

Table 1
Parameters of DSC curves for various samples.

Sample	T_{pI} (°C)	T_{pII} (°C)	ΔH_{cI} (J/g)	ΔH_{cII} (J/g)
B1 (PTT)	176.4	–	−50.4	–
B2 (PET20/PTT80)	192.4	–	−46.0	–
B3 (PET40/PTT60)	193.2	–	−44.9	–
B4 (PET60/PTT40)	198.5	208.3	−39.3[a]	−34.0[a]
B5 (PET80/PTT20)	198.5	212.9	−33.5[a]	−37.0[a]
B6 (PET100)	–	192.6	–	−23.5

[a]Normalized for PTT and PET contents, respectively.

For both binary blends of B2 (PET20/PTT80) and B3 (PET40/PTT60), as PET component is the minor one in blends, only a single crystallization exotherm is observed in each DSC curve. Moreover, it can be found that the crystallization peak temperature (192.4 °C for B2, 193.2 °C for B3) is much higher than that of pure PTT (176.4 °C) while it is closed to that of pure PET (192.6 °C). It should be noted that PET and PTT will crystallize individually and successively, although only one peak is observed. As the blend melt was cooled, the PET component with higher supercooling degree will crystallize first, and then the crystallite of PET will be the nucleating agent for PTT, which will greatly improve the crystallization of PTT at a higher temperature. Moreover, the crystallization peaks of B2 and B3 are stronger and sharper than that of B1, indicating a faster crystallization rate of the blends. These results suggest that the commingled minor addition of the PET to PTT helps to improve the crystallization of the blends.

While in the DSC curves of B4 (PET60/PTT40) and B5 (PET80/PTT20), as PET component is the major one in blends, two crystallization exothermal peaks are clearly observed: the primary II and subordinate I, which is different to the literatures [5]. Peaks II and I are attributed to the crystallization behavior of PET and PTT, respectively, according to their crystallization temperatures. By careful observation, it is found that the temperature of peak II is much higher than that of neat PET, and peak I is much higher than that of neat PTT. The peak II shifting to higher temperature could be attributed to the diluent effect of PTT in the melt, which increase the mobility of PET molecular segments and improve the crystallization of PET molecules. The peak I shifting to higher temperature could be due to the crystallized PET, which act as nucleating agent and induce the crystallization of PTT at subsequent higher temperature. Furthermore, it can be seen in Table 1 that ΔH_{cI} and ΔH_{cII} are varied with the blends composition. For B2 and B3 blends, the values of ΔH_{cI} cannot be normalized for PTT and PET contents because the percentage of PET that crystallizes together with PTT is unknown. However, judging from their crystallization temperatures of peak I, we believe that peak I is predominant for the crystallization of PTT. Because there are two crystallization peaks in B4 and B5 blends, the crystallization enthalpy can be normalized for PTT and PET contents, respectively. Due to the PET component is the major component in B4 and B5 blends, ΔH_{cI} for PTT is decreased while ΔH_{cII} for PET is increased as PET content increasing. On the other hand, ΔH_{cII} of B4 and B5 is much higher than that of B6 (PET), suggesting that the dilute effect of PTT is great, which highly improve the crystallization of PET. Thus, it can be concluded that each component of the blends are positive to promote the crystallization of another one.

3.2. Isothermal crystallization kinetics

3.2.1. Isothermal crystallization behaviors

The exothermal diagrams of isothermal crystallization analysis for B1–B3 are shown in Fig. 2(a)–(c). As the crystallization temperature (T_c) increased, the exothermal peaks of each curve shift to longer time, indicating that a progressively slower crystallization rate as T_c increases. From the data listed in Table 2, the crystallization enthalpy (ΔH_c) of each sample gradually increases with T_c. Moreover, comparing the isothermal crystallization enthalpy of B2 and B3 with that of neat PTT, it is clear that the more the PET content in binary blend, the less the ΔH_c is.

Table 2
Parameters of isothermal crystallization curves for various samples.

Sample	T_c (°C)	$t_{1/2}$ (min)	t_c (min)	n	Z_t (min^{-n})	ΔH_c (J/g)
B1	194	6.38	15.25	2.1	133.7×10^{-4}	−45.0
	196	9.24	20.75	2.4	31.2×10^{-4}	−46.6
	198	12.45	26.15	2.6	10.2×10^{-4}	−48.0
	200	17.13	36.35	2.6	4.4×10^{-4}	−48.8
	202	22.75	44.45	2.6	2.2×10^{-4}	−48.9
B2	194	0.38	1.40	2.9	19.4	−28.3
	196	0.59	2.68	3.0	7.3	−30.1
	198	0.86	3.96	3.0	1.4	−31.5
	200	1.23	5.40	3.0	0.4	−33.1
	202	1.65	6.80	3.0	0.2	−35.2
B3	194	0.28	1.02	2.9	32.7	−27.2
	196	0.42	1.78	3.0	15.7	−28.9
	198	0.64	3.78	3.0	3.7	−31.7
	200	0.92	3.84	3.0	1.0	−32.8
	202	1.25	4.80	3.0	0.4	−34.7

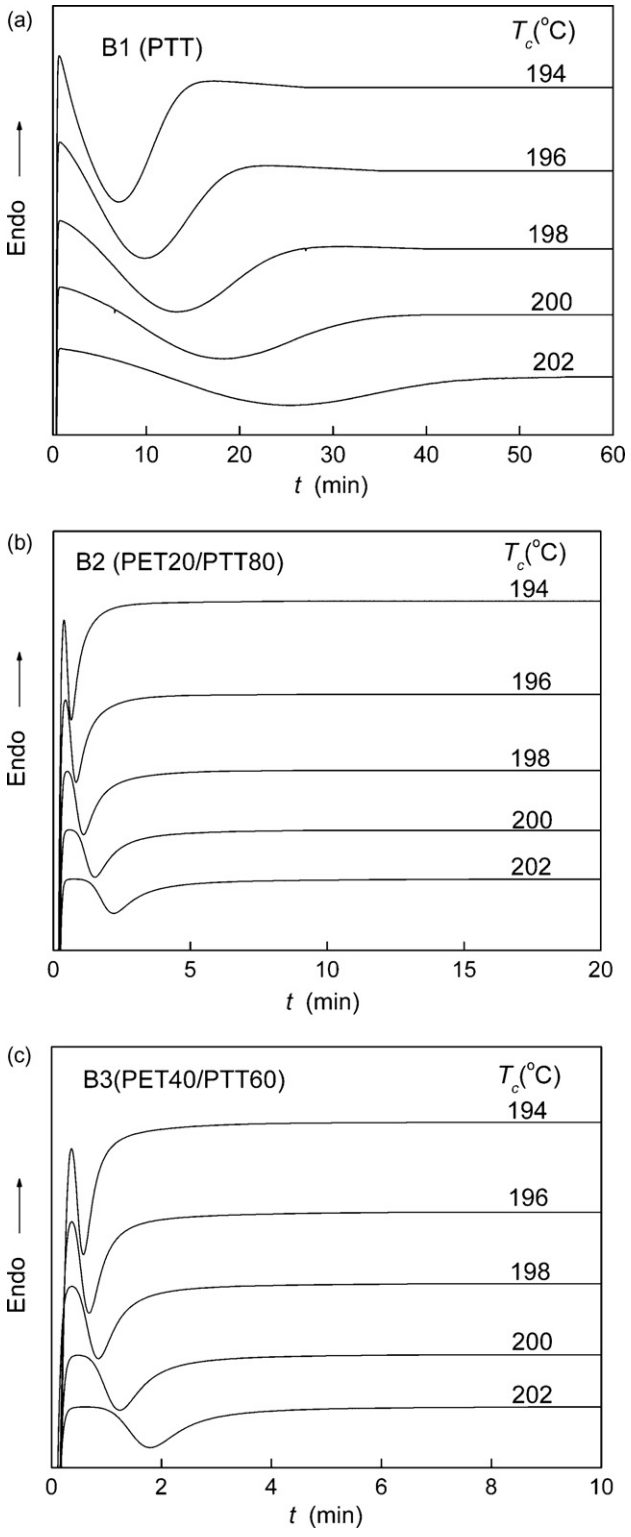

Fig. 2. Heat flow versus time during isothermal crystallization of (a) B1 and (b) B2 samples at designated crystallization temperatures.

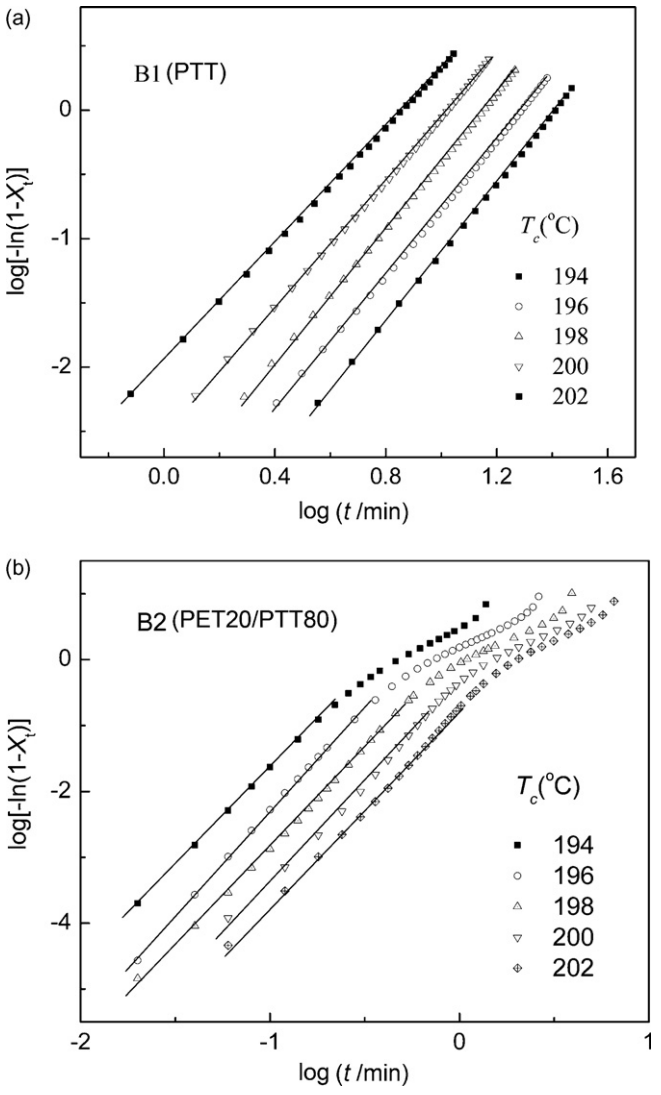

Fig. 3. Plots of $\log[-\ln(1 - X_c(t))]$ versus $\log t$ for isothermal crystallization of (a) B1 and (b) B2 blends at indicated temperatures.

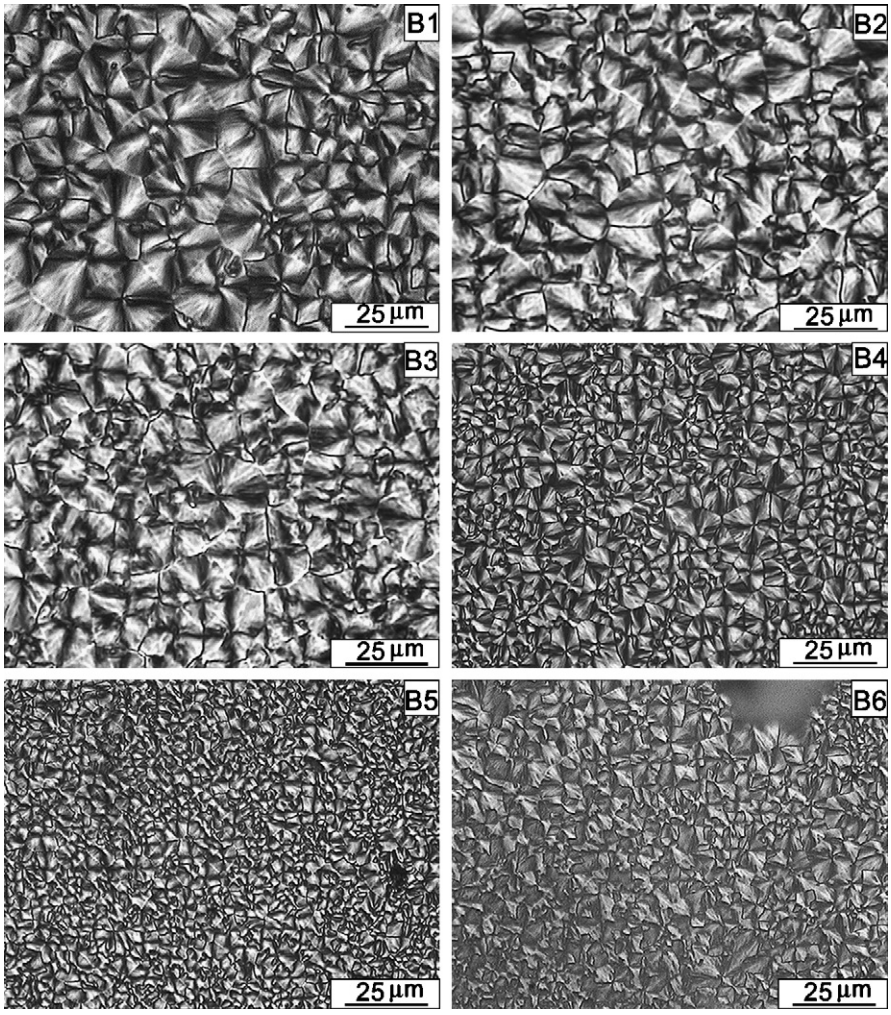

Fig. 4. Polarized optical microscopic pictures of all blends isothermally crystallized at 200 °C.

Another important parameter is the half-time of crystallization ($t_{1/2}$), which is defined as the time taken from the onset of the relative crystallinity until 50% completion. The dependence of $t_{1/2}$, as well as the t_c (total crystallization time from beginning to finishing), upon T_c for B1, B2 and B3 samples are listed in Table 2. It is seen that $t_{1/2}$ and t_c of the neat PTT increases much as T_c increases from 194 to 202 °C; whereas for B2 and B3 blends they are shown slowly increasing with increasing T_c. Comparing the $t_{1/2}$ or t_c of B1 with that of B2 and B3, the blends have much smaller crystallization time; moreover, the more the PET content in blends, the less the $t_{1/2}$ or t_c is. Thus, it can be concluded that the minor commingled addition of PET component to PTT molecules greatly increases the crystallization of the blends (the reason will be discussed later).

3.2.2. Analysis based on the Avrami equation

Assuming that the relative crystallinity ($X_c(t)$) increases with the crystallization time (t), the Avrami equation can be used to analyze the isothermal crystallization process of the neat PTT and B2, B3 blends as follows [19,20]:

$$1 - X_c(t) = \exp(-Z_t t^n) \quad (1)$$

$$\log[-\ln(1 - X_c(t))] = n \log t + \log Z_t \quad (2)$$

where $X_c(t)$ is the relative crystallinity at time t; the exponent n is a mechanism constant with a value depending on the type of nucleation and the growth dimension, and the parameter Z_t is a growth rate constant involving both nucleation and the growth rate parameters.

The plots of $\log[-\ln(1 - X_c(t))]$ versus $\log t$ according to Eq. (2) are shown in Fig. 3(a) and (b). For pure PTT, most of the experimental data is in good linear relationship. However, the curves of B2 and B3 are all composed of two linear sections. This fact indicates that the secondary crystallization is obvious in the PET/PTT blends. Here, the observed slow crystallization for B2 and B3 can be considered that secondary crystallization occurs in amorphous regions constrained by the close crystalline regions, which can produce a lowering of the crystallization rate.

The Avrami exponent n and the rate constant Z_t can readily be extracted from the Avrami plots of Fig. 3. The values of n and Z_t of all samples are listed in Table 2. In this work, the values of n for pure PTT is found to range from 2.1 to 2.6 in the temperature range, which, according to the definition of the Avrami exponent [21–25] and the crystal morphology in Fig. 4, may correspond to a two-dimensional growth at 194 °C, and a three-dimensional growth at 196–202 °C during the whole crystallization time with an athermal nucleation mechanisms.

The values of n for B2 and B3 are about 3.0 for the primary crystallization stage. In these binary blends, minor content of PET can crystallize at a higher temperature, and then the crystallized PET acts as seeds for the crystal growth of PTT; thus the mechanism of crystal growth is heterogeneous nucleation for PTT in blends. As a result, their growth dimension should mostly be three-dimensional

space extension for the primary crystallization. This can be demonstrated by the crystal morphology in Fig. 4.

Another overall rate parameter (Z_t) which determines both the nucleating and the growth process is extremely sensitive to temperature for each sample, that is, the higher the crystallization temperature, the lower the crystallization rate. Comparing the value Z_t of B1 with those of B2 and B3 at the same T_c, it is clear that B2 and B3 have a much higher crystallization rate, indicating that the crystallization rate is greatly increased with minor content of PET agents in blends. Z_t of B3 is also higher than that of B2 at the same T_c. Generally speaking, there are two factors make contribution to the increasing of crystallization rate: one is the flexible of the molecular chains, i.e., the more flexible the polymer chain, the faster the crystallization rate; the other is the ability of nucleation, the higher the ability of nucleation, the faster the crystallization rate both at low and high temperature. The PET component, which has higher T_m and under higher supercooling situation compared with PTT [18], can crystallize at a higher temperature and act as the nucleating sites where PTT could be easily nucleated. The crystallization rate consists of nucleation and growth rates; since both of the two factors are improved, the crystallization rate is greatly increased.

As seen in Table 2, the crystallization exothermal enthalpy of B1 is much higher than those of B2 and B3. Although the values of ΔH_c should be normalized for PTT and PET contents, respectively, the percentage of PET that crystallizes together with PTT is unknown in the blends of B2 and B3. Therefore, only the total crystallization enthalpy can be used to evaluate the blends crystallinity. ΔH_c results suggest that the blends have a much lower crystallinity than pure PTT.

In order to demonstrate the crystal growth geometry of the blends, the crystal morphology of PTT, PET and the blends annealed at T_c = 200 °C are obtained under POM, as shown in Fig. 4 (B1)–(B6). Fig. 4 (B1) reveals well-defined large spherulitic of pure PTT, and spherulites impinge on each other forming polygonal spherulites with the clear boundaries; while Fig. 4 (B6) of pure PET gives some defective Maltese cross of the poor crystal morphology. As seen from Fig. 4 (B2)–(B5), with increasing contents of PET in blends, spherulites' size gradually decreases. These results are consisted with the conclusions deduced from the Avrami analysis on the isothermal crystallization: firstly, the nucleation mode of the blends is heterogeneous and the crystal is three-dimensional growth in blends; secondly, the crystallization of the blends is faster than PTT, therefore, more spherulites will form with smaller size in a limited space.

3.2.3. *Melting behavior of the samples annealed at different temperatures*

Fig. 5(a) and (b) presents a series of DSC heating thermograms for B2 and B3 blends that had been annealed at different T_c. DSC melting parameters are listed in Table 3. As seen in Fig. 5 and Table 3, both the melting endotherms of B2 and B3 show a small melting peak (I) and two large melting peaks (II and III). Peaks I and II shift to higher temperature as T_c increases from 194 to 202 °C, but peak III changes little. Multiple-melting phenomenon of PET [26–29] and PTT [30–34] has previously been reported.

Table 3
Melting parameters of various samples.

Sample	T_c (°C)	T_{mI} (°C)	ΔH_{mI} (J/g)	T_{mII} (°C)	T_{mIII} (°C)
B2	194	201.3	1.58	213.3	223.2
	196	204.0	1.60	214.8	223.7
	198	205.9	1.64	216.3	223.8
	200	207.7	1.71	218.0	224.0
	202	210.0	1.76	219.4	223.9
B3	194	201.6	1.62	213.8	223.3
	196	203.7	1.65	215.2	223.8
	198	205.7	1.68	216.8	224.0
	200	207.5	1.74	218.5	224.0
	202	209.6	1.79	220.0	224.1

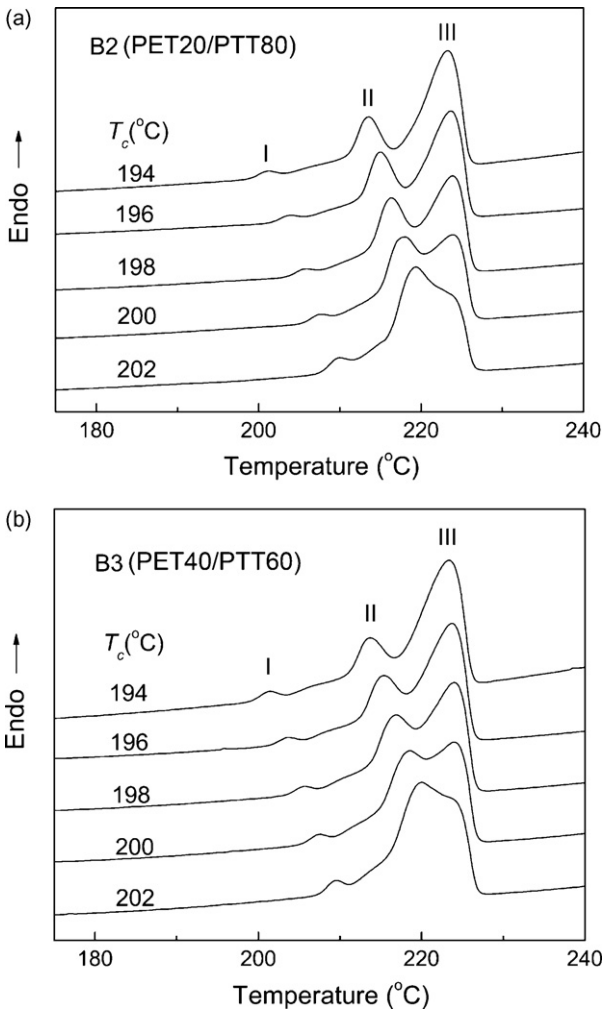

Fig. 5. Melting endotherms of (a) B2 and (b) B3 blends recorded at a heating rate of 10 °C/min after isothermal crystallization at the specified temperatures.

Commonly, the melting peaks of PET component in blends appear in the temperature range of 230–260 °C, however, no peaks are observed in this temperature range in both Fig. 5(a) and (b) in this study. This result may due to three reasons: one is because of the minor PET component in binary blends; the second is that PET form only some micro-crystallites during the isothermal crystallization process; the last may because both PET and PTT components may form stereo-complex crystals during the isothermal crystallization process, which may melt at a lower temperature during heating process and the peaks are overlapped by other melting peaks at a lower temperature.

The origin of the small endotherm (peak I), generally observed a few degrees above the crystallization temperature in many polymers, is a widely discussed matter [35–40]. The most frequent interpretation considers it the result of partial fusion with superposition of a recrystallization process even if it has also been proposed that it can originate from enthalpic recovery connected to mobilization of the rigid amorphous fraction. Wunderlich [37] and Righetti [38] studied the origin of low-temperature endotherm of PET and PTT by modulated differential scanning calorimetry (TMDSC), respectively. They believe that the origin of the endotherm is connected with both partial fusion of the crystalline portions and

enthalpy recovery subsequent to structural relaxation of the rigid amorphous fraction. Recently, Schick [39] also suggest the same conclusion on the low-temperature endotherm of polystyrene. In Fig. 5(a) and (b), the multiple-melting peaks of B2 and B3 blends are interpreted as follows: at the low heating rate (10 °C/min), peak I is originated from both of the melting of the originally formed crystals and the RAF relaxation; peaks II and III are the remelting of the recrystallized crystals.

In Table 3, the melting enthalpy (ΔH_{ml}) are about 1.6–1.8 J/g. However, as shown in Table 2, the crystallization enthalpies (ΔH_c) are about ~30 J/g in the isothermal crystallization process. The data value difference between ΔH_{ml} and ΔH_c is very large. This can be explained clearly by the conclusions of the previous research works [39,40]. They suggest that as soon as some crystals are molten they recrystallize. The total enthalpy change is close to zero because melting and crystallization enthalpies are nearly the same. If melting and crystallization are compensating each other there is no effect in heat capacity (heat flow rate) and the DSC curve is essentially flat (without peaks). When the difference between the melting rate and recrystallization rate is maximal, a peak appears. Therefore, the reorganization starts already just after the beginning of the melting at low temperature. As the T_c increasing form 194 to 202 °C, peak I increases from 201 to 210 °C; this may be explained by the difference in crystal stability (melting points), i.e., the crystals formed at higher T_c has the higher stability. On the other hand, peaks II and III have a trend to fuse each other and peak III becomes smaller and smaller at higher T_c (e.g. 202 °C); this may be explained that the recrystallization rate become lower at higher temperature, so that the reorganization will be decreased.

4. Conclusion

PET/PTT blends prepared by melt-blending are investigated on its melt-crystallization, isothermal crystallization kinetics and crystals' morphology. When the blends were cooled from melt, PET and PTT crystallize individually, but they influenced each other: PTT is a dilute agent for PET to crystallize while the crystallized PET acts as a nucleating agent for the crystallization of PTT at high temperature. The Avrami exponent n and Z_t calculated from the Avrami equation indicate different crystallization mechanisms occurred in blends compared with pure PTT, and the crystallization rate is greatly increased in blends. The crystal growth dimension of the blends is mainly three-dimensional growth during the designated isothermal crystallization process, but the spherulites' size is much smaller than those formed in pure PTT. On the whole, the commingled minor addition of one component to another helps to improve the crystallization of the blends.

Acknowledgement

The work is supported by the financial support from the Natural Science Foundation of Hebei Province (B2007000148) and Hebei University (Y2006065), PR China.

References

[1] D.R. Paul, C.B. Bucknall, Polymer Blends, Wiley–InterScience, 2000.
[2] L.A. Utracki, Polymer Blends Handbook, Kluwer Academic, Netherlands, 2003.
[3] H.A. Khonakdar, S.H. Jafari, A. Asadinezhad, Iran. Polym. J. 17 (2008) 19–38.
[4] J. Wu, J.M. Schultz, J.M. Samon, A.B. Pangelinan, H.H. Chuah, Polymer 42 (2001) 7141–7151.
[5] P. Supaphol, N. Dangseeyun, P. Thanomkiat, M. Nithitanakul, J. Polym. Sci., Part B: Polym. Phys. 42 (2004) 676–686.
[6] Y.H. Kuo, M. Woo, Polym. J. 35 (2003) 236–244.
[7] M. Castellano, A. Turturro, B. Valenti, A. Avagliano, G. Costa, Macromol. Chem. Phys. 207 (2006) 242–251.
[8] C.Y. Ko, M. Chen, H.C. Wang, I.M. Tseng, Polymer 46 (2005) 8752–8762.
[9] C.Y. Ko, M. Chen, C.L. Wang, H.C. Wang, R.Y. Chen, I.M. Tseng, Polymer 48 (2007) 2415–2424.
[10] E. Ponnusamy, T. Balakrishnan, J. Macromol. Sci. Chem. A22 (1985) 373–378.
[11] E. Ponnusamy, T. Balakrishnan, Polym. J. 17 (1985) 473–477.
[12] J.W. Lee, S.W. Lee, B. Lee, M. Ree, Macromol. Chem. Phys. 202 (2001) 3072–3080.
[13] T.M. Wu, Y.W. Lin, J. Polym. Sci., Part B: Polym. Phys. 42 (2004) 4255–4271.
[14] G.F. Wei, L.Y. Wang, G.K. Chen, L.X. Gu, J. Appl. Polym. Sci. 100 (2006) 1511–1521.
[15] T.W. Shyr, C.M. Lo, S.R. Ye, Polymer 46 (2005) 5284–5298.
[16] T. Kiyotsukuri, T. Masuda, N. Tsutsumi, Polymer 35 (1994) 1274–1279.
[17] M.T. Run, Y.J. Wang, C.G. Yao, J.G. Gao, Thermochim. Acta 447 (2006) 13–21.
[18] M.T. Run, A.J. Song, Y.J. Wang, C.G. Yao, J. Appl. Polym. Sci. 104 (2007) 3459–3468.
[19] M. Avrami, J. Chem. Phys. 8 (1939) 212–224.
[20] M. Avrami, J. Chem. Phys. 9 (1941) 177–184.
[21] B. Wunderlich, Macromolecular Physics, vol. 2, Academic Press, New York, 1976, p. 132.
[22] F.C. Pérez-ćardenas, L.F. Del Castillo, R. Vera-Graziano, J. Appl. Polym. Sci. 43 (1991) 779–782.
[23] S. Liu, Y. Yu, Y. Cui, H. Zhang, Z. Mo, J. Appl. Polym. Sci. 70 (1998) 2371–2380.
[24] P. Supaphol, J.E. Spruiell, J. Appl. Polym. Sci. 75 (2000) 337–346.
[25] H. Janeschitz-Kriegl, E. Ratajski, H. Wippel, Colloid. Polym. Sci. 277 (1999) 217–226.
[26] G.E. Sweet, J.P. Bell, J. Polym. Sci. A-2 10 (1972) 1273–1283.
[27] X.F. Lu, J.N. Hay, Polymer 42 (2001) 9423–9431.
[28] Y. Kong, J.N. Hay, Polymer 44 (2003) 623–633.
[29] A.A. Minakov, D.A. Mordvintsev, C. Schick, Polymer 45 (2004) 3755–3763.
[30] P.L. Wu, E.M. Woo, J. Polym. Sci., Part B: Polym. Phys. 41 (2003) 80–86.
[31] W.T. Chung, W.J. Yeh, P.D. Hong, J. Appl. Polym. Sci. 83 (2002) 2426–2433.
[32] P. Srimoaon, N. Dangseeyun, P. Supaphol, Eur. Polym. J. 40 (2004) 599–608.
[33] N. Dangseeyun, P. Srimoaon, P. Supaphol, M. Nithitanakul, Thermochim. Acta 409 (2004) 63–77.
[34] N. Apiwanthanakorn, P. Supaphol, M. Nithitanakul, Polym. Test. 23 (2004) 817–826.
[35] M. Song, J. Appl. Polym. Sci. 81 (2001) 2779–2785.
[36] H. Xu, B.S. Ince, P. Cebe, J. Polym. Sci., Polym. Phys. 41 (2003) 3026–3036.
[37] B. Wunderlich, J. Polym. Sci., Polym. Phys. 36 (1998) 2499–2511.
[38] M.C. Righetti, M.L. Lorenzo, E. Tombari, M. Angiuli, J. Phys. Chem. B 112 (2008) 4233–4241.
[39] A.A. Minakov, D.A. Mordvintsev, T. Rob, C. Schick, Thermochim. Acta 442 (2006) 25–30.
[40] M.C. Righetti, M.L. Di Lorenzo, J. Polym. Sci., Polym. Phys. 42 (2004) 2191–2201.